

# Less is More: Contextual Sampling for Nonlinear Data-Enabled Predictive Control

Julius Beerwerth<sup>1</sup> and Bassam Alrifaae<sup>1</sup>

**Abstract**—Data-enabled Predictive Control (DeePC) is a powerful data-driven approach for predictive control without requiring an explicit system model. However, its high computational cost limits its applicability to real-time robotic systems. For robotic applications such as motion planning and trajectory tracking, real-time control is crucial. Nonlinear DeePC either relies on large datasets or learning the nonlinearities to ensure predictive accuracy, leading to high computational complexity. This work introduces contextual sampling, a novel data selection strategy to handle nonlinearities for DeePC by dynamically selecting the most relevant data at each time step. By reducing the dataset size while preserving prediction accuracy, our method improves computational efficiency, of DeePC for real-time robotic applications. We validate our approach for autonomous vehicle motion planning. For a dataset size of 100 sub-trajectories, Contextual sampling DeePC reduces tracking error by 53.2% compared to Leverage Score sampling. Additionally, Contextual sampling reduces max computation time by 87.2% compared to using the full dataset of 491 sub-trajectories while achieving comparable tracking performance. These results highlight the potential of Contextual sampling to enable real-time, data-driven control for robotic systems.

**Video:** <https://bassamlab.github.io/DeePC-Contextual-Sampling/>

## I. INTRODUCTION

Real-time control of nonlinear robotic systems is critical for applications such as autonomous navigation, robotic manipulation, and aerial robotics. Model Predictive Control (MPC) is widely used in robotic motion planning and control due to its ability to handle constraints and optimize performance [1]. However, deploying MPC in real-world robotic applications often requires an accurate system model, which may be unavailable or computationally expensive to maintain. This limitation is particularly critical for autonomous vehicle racing, where achieving precise trajectory tracking, high-speed stability, and dynamic adaptation requires accurate modeling of complex vehicle dynamics [2], [3]. Model inaccuracies can lead to suboptimal lap times or instability, making real-time control a significant challenge.

To address the challenges related to model dependency, several data-driven control approaches have been proposed, offering alternatives to traditional model-based methods. These approaches leverage input-output data to learn system behavior, bypassing the need for explicit model identification. Among these approaches, Data-enabled Predictive Control

(DeePC) [4] has garnered attention due to its ability to optimize system performance while respecting constraints. DeePC directly incorporates control objectives and system constraints into its formulation, making it particularly appealing for practical applications. However, its computational demands remain a key limitation when dealing with large datasets or highly nonlinear systems.

In this work, we propose an efficient data selection strategy for DeePC, called Contextual Trajectory sampling, which dynamically selects the most relevant data based on the robot's current state. By reducing the dataset size, our method enables real-time predictive control while maintaining high tracking accuracy. We validate our approach in the context of motion planning for autonomous vehicles.

Related work has explored various approaches to data-driven control. In [5], Berberich and Allgöwer provide an overview of data-driven control with a focus on system-theoretic guarantees. They divide data-driven approaches for nonlinear systems into two classes: (1) approaches that exploit global linearity in higher-dimensional coordinates and (2) approaches that exploit local linearity of nonlinear systems.

The first class of approaches assume structural knowledge of nonlinearities or attempts to learn them. [6] extends a data-driven framework to Hammerstein-Wiener systems, showing that unknown nonlinearities can be approximated via kernel methods. Similarly, [7] presents a data-driven internal model controller for second-order discrete Volterra systems. Both methods do not consider output nonlinearities. To address this, [8] introduces a simulation approach for Nonlinear Autoregressive Exogenous (NARX) systems, covering various nonlinear models, including Gaussian Processes and Neural Networks.

Other strategies aim to lift system dynamics into higher-dimensional representations. [9] and [10] use reproducing kernel functions and the Koopman operator, respectively, enabling globally linear dynamics but increasing optimization complexity. An alternative strategy in [11] integrates regularized kernel methods with DeePC to capture nonlinearities via the representer theorem, introducing a structured yet nonconvex optimization problem. Further extending DeePC, [12] incorporates general basis functions, proposing sparse regularization and ridge regression for computational efficiency. [13] advances this with neural networks to learn implicit nonlinear bases, offering more flexibility. These works extend DeePC by embedding prior system knowledge (kernel methods, basis functions) or enabling purely data-driven representations (neural networks).

The second class of approaches leverage the fact that nonlin-

<sup>1</sup> The authors are with the Department of Aerospace Engineering, University of the Bundeswehr Munich, Germany, [firstname].[lastname]@unibw.de

ear systems can be locally approximated by linear dynamics. [14] extends Willems' Fundamental Lemma to affine systems, proposing an approach that updates data online for accurate local predictions. However, this requires persistently exciting input signals to ensure sufficient system exploration. These approaches either assume system structure, increase computational complexity, or impose additional input constraints. Moreover, their real-time feasibility is often not explored. In contrast, this work builds on [15] by dynamically selecting the most relevant data points rather than sampling from a fixed dataset, reducing computational cost while maintaining predictive accuracy.

Our proposed method overcomes these limitations by selecting trajectories near the current operating point, avoiding the need for global approximations while ensuring real-time efficiency.

## II. METHODOLOGY

*Notation:* We denote by  $\text{col}(\cdot)$  the column-wise concatenation of vectors or matrices,  $\text{colspan}(\cdot)$  the column space of a matrix, and  $\|\cdot\|_R$  the weighted 2-norm with weighting matrix  $R$ .

### A. Preliminaries

DeePC [4] is based on Behavioral Systems Theory [16] for discrete-time linear time-invariant (LTI) systems whose input-output trajectories satisfy Willems' Fundamental Lemma [17], meaning that all valid trajectories can be reconstructed from a sufficiently rich set of past data.

**Definition 1** (Persistency of Excitation, [4], [17]). *Let  $L, T \in \mathbb{Z}_{>0}$  such that  $T \geq L$ . A signal  $u = \text{col}(u_1, \dots, u_T) \in \mathbb{R}^{Tm}$  is persistently exciting of order  $L$  if the Hankel matrix*

$$\mathcal{H}_L(u) := \begin{bmatrix} u_1 & u_2 & \cdots & u_{T-L+1} \\ u_2 & u_3 & \cdots & u_{T-L+2} \\ \vdots & \vdots & \ddots & \vdots \\ u_L & u_{L+1} & \cdots & u_T \end{bmatrix} \quad (1)$$

is of full row rank.  $\square$

Here,  $T$  represents the length of the signal and  $m$  the number of inputs. In other words, a *persistently exciting* signal excites the system such that the resulting input/output signal captures the whole system behavior. This condition bounds the length of the trajectory to  $T \geq (m+1)L - 1$ . Subsequently, the Fundamental Lemma states that the columns of the Hankel matrix span a subspace equal to the subspace of trajectories the underlying linear system can generate. We refer to the columns of the Hankel matrix as sub-trajectories.

**Lemma 1.** (Fundamental Lemma, [4], [17]) *Consider a controllable system  $\mathcal{B}$ . Let  $T, t \in \mathbb{Z}_{>0}$ , and  $w = \text{col}(u, y) \in \mathcal{B}_T$ . Assume  $u$  to be persistently exciting of order  $t + \mathbf{n}(\mathcal{B})$ . Then*

$$\text{colspan}(\mathcal{H}_t(w)) = \mathcal{B}_t.$$

$\mathcal{B}_T$  represents the set of trajectories truncated to length  $T$ , and  $\mathbf{n}(\mathcal{B})$  the order of the minimal input/output/state

representation of the underlying linear system. Extensions of the Fundamental Lemma relax the assumption on the structure of the data matrix from the original Hankel matrix to Page matrices [18] and to mosaic-Hankel matrices [19], given that the input sequences are *collectively persistently exciting* of order  $t + \mathbf{n}(\mathcal{B})$ , meaning the mosaic-Hankel matrix  $\tilde{\mathcal{H}}_L$  has full row rank. A mosaic-Hankel matrix is a horizontal concatenation of multiple Hankel matrices. The latter extension is essential for our approach, as it allows us to select a subset of the original Hankel matrix.

To leverage the Fundamental Lemma, given the mosaic-Hankel matrix  $\tilde{\mathcal{H}}_L$  we build the input and output Hankel matrices  $\tilde{\mathcal{H}}_L(u), \tilde{\mathcal{H}}_L(y)$ . These are then partitioned into past and future data of length  $L = T_{\text{ini}} + N$ , respectively:

$$\begin{pmatrix} \tilde{U}_p \\ \tilde{U}_f \end{pmatrix} := \tilde{\mathcal{H}}_{T_{\text{ini}}+N}(u), \quad \begin{pmatrix} \tilde{Y}_p \\ \tilde{Y}_f \end{pmatrix} := \tilde{\mathcal{H}}_{T_{\text{ini}}+N}(y). \quad (2)$$

According to the Fundamental Lemma, the trajectory  $\text{col}(u_{\text{ini}}, y_{\text{ini}}, u, y)$  belongs to the linear system  $\mathcal{B}_{T_{\text{ini}}+N}$  if and only if there exists  $g$  such that:

$$\begin{pmatrix} \tilde{U}_p \\ \tilde{Y}_p \\ \tilde{U}_f \\ \tilde{Y}_f \end{pmatrix} g = \begin{pmatrix} u_{\text{ini}} \\ y_{\text{ini}} \\ u \\ y \end{pmatrix}. \quad (3)$$

The signals  $u_{\text{ini}}, y_{\text{ini}}$  represent the last  $T_{\text{ini}}$  initial inputs and outputs and  $u, y$  the future inputs and outputs. The first three blocks of equation (3) can be solved for  $g$ , given  $u_{\text{ini}}, y_{\text{ini}}$ , and  $u$ . The future outputs can be predicted by solving the last block of equation (3)  $\tilde{Y}_f g = y$ .

### B. Regularized DeePC

In DeePC, this data-driven predictor is used as a nonparametric model. At each time step, optimization problem (4) is solved in a receding horizon fashion to compute the optimal inputs in terms of the given cost function. Our approach is based on the regularized formulation of DeePC:

$$\begin{aligned} & \underset{g, u, y, \sigma_y}{\text{minimize}} && \sum_{k=1}^N \|y_k - r_k\|_Q^2 + \sum_{k=0}^{N-1} (\|u_k\|_R^2 + \|\Delta u_k\|_R^2) \\ & && + \lambda_g \|g\|_2 + \lambda_\sigma \|\sigma_y\|_2 + \lambda_\sigma \|\sigma_u\|_2, \\ & \text{subject to} && \begin{pmatrix} \tilde{U}_p \\ \tilde{Y}_p \\ \tilde{U}_f \\ \tilde{Y}_f \end{pmatrix} g = \begin{pmatrix} u_{\text{ini}} \\ y_{\text{ini}} \\ u \\ y \end{pmatrix} + \begin{pmatrix} \sigma_u \\ \sigma_y \\ 0 \\ 0 \end{pmatrix}, \\ & && u_k \in \mathcal{U}, \quad \forall k \in \{0, \dots, N-1\}, \\ & && y_k \in \mathcal{Y}, \quad \forall k \in \{1, \dots, N\}. \end{aligned} \quad (4)$$

The cost function consists of a tracking term to follow the reference  $r$ , a penalty on  $u$  to minimize energy, a penalty on  $\Delta u$  for smooth input trajectories, and two regularization terms. We use the 2-norm instead of the 1-norm for regularization, as it is computationally more efficient [15]. The regularization on

$g$  enables reliable performance for noisy data, while the regularization on the slack variable  $\sigma_y$  is intended as a penalty. The data-driven predictor is incorporated as an equality constraint describing the relation between  $u$  and  $y$ . Note that a slack variables  $\sigma_u$  and  $\sigma_y$  were added to ensure that the constraint is feasible in the case of nonlinear data. Last, constraints on  $u$  and  $y$  are encoded in the sets  $\mathcal{U}$  and  $\mathcal{Y}$ , respectively. Note that the data matrices have mosaic-Hankel structure and can be build from a subset of sub-trajectories.

### C. Contextual Sampling

We propose the use of Contextual sampling to address two issues. First, the number of sub-trajectories in the Hankel matrix is equivalent to the length of  $g$ . As a consequence the number of optimization variables in the optimization problem increases with the size of the Hankel matrix, leading to greater computational complexity. Second, while approximating the system dynamics of a nonlinear system via (3) works well for various applications [4], [15], there is still room for improvement, as shown by numerous works extending DeePC for nonlinear systems [9], [11]–[13].

Contextual sampling addresses these issues by selecting the data closest to the current initial output trajectory, thus reducing the amount of data used for prediction and staying close to the current dynamics. At each time step, we identify past trajectories that are closest to the current operating point. Given  $(u_{\text{ini}}, y_{\text{ini}})$ , we define the distance to each sub-trajectory  $(U_{p,i}, Y_{p,i})$  in the past Hankel matrices as:

$$d_i = \|W((u_{\text{ini}}, y_{\text{ini}}) - (U_{p,i}, Y_{p,i}))\|_2, \quad (5)$$

where  $W$  is a block-diagonal scaling matrix:

$$W = \text{diag} \left( \frac{1}{\sigma_{u_1}}, \dots, \frac{1}{\sigma_{u_m}}, \dots, \frac{1}{\sigma_{y_1}}, \dots, \frac{1}{\sigma_{y_p}}, \dots \right), \quad (6)$$

with each standard deviation  $\sigma_{u_j}$  and  $\sigma_{y_k}$  computed across all available data. This ensures that all state and control variables contribute equally to the distance measure. While individual sub-trajectories of  $Y_p$  may not perfectly match  $y_{\text{ini}}$ , the selected subset spans a subspace that approximates the current system behavior. We extract the  $N_s$  indices of the smallest entries of  $d$  and store them in the set  $\mathcal{I}$ :

$$\mathcal{I} = \underset{|\mathcal{I}|=N_s}{\text{argmin}} \sum_{i \in \mathcal{I}} d_i. \quad (7)$$

The number of sampled sub-trajectories  $N_s$  is a tuning parameter. We want to keep it as small as possible, but as large as necessary. In Section III-B, we will observe that choosing  $N_s$  creates a trade-off between computation time and tracking accuracy.

Using the selected sub-trajectory indices  $\mathcal{I} = \{\dot{i}_1, \dot{i}_2, \dots, \dot{i}_{N_s}\}$ , we construct the mosaic-Hankel matrices  $\tilde{U}_p, \tilde{Y}_p, \tilde{U}_f, \tilde{Y}_f$  from the original Hankel matrices  $U_p, Y_p, U_f, Y_f$ :

$$\begin{aligned} \tilde{U}_p &= U_{p,:\mathcal{I}}, & \tilde{Y}_p &= Y_{p,:\mathcal{I}}, \\ \tilde{U}_f &= U_{f,:\mathcal{I}}, & \tilde{Y}_f &= Y_{f,:\mathcal{I}}. \end{aligned} \quad (8)$$

This process is repeated at every time step to adapt the data to the current operating point. We outline the combination of Contextual sampling and DeePC in Algorithm 1.

---

#### Algorithm 1 DeePC with Contextual sampling

---

**Input:** Hankel matrices  $\{U_p, Y_p, U_f, Y_f\}$ , reference trajectory  $r$ , past input/output data  $\{u_{\text{ini}}, y_{\text{ini}}\}$  of length  $T_{\text{ini}}$ , constraint sets  $\mathcal{U}$  and  $\mathcal{Y}$ , performance weights  $Q$  and  $R$ , number of samples  $n_s$ .

- 1: **Compute distance vector:**

$$d_i = \|W((u_{\text{ini}}, y_{\text{ini}}) - (U_{p,i}, Y_{p,i}))\|_2,$$

- 2: **Extract closest trajectories:**

$$\mathcal{I} = \underset{|\mathcal{I}|=n_s}{\text{argmin}} \sum_{i \in \mathcal{I}} d_i$$

- 3: **Construct mosaic-Hankel matrices:**

$$\begin{aligned} \tilde{U}_p &= U_{p,:\mathcal{I}}, & \tilde{Y}_p &= Y_{p,:\mathcal{I}}, \\ \tilde{U}_f &= U_{f,:\mathcal{I}}, & \tilde{Y}_f &= Y_{f,:\mathcal{I}} \end{aligned}$$

- 4: **Solve** (4) for  $g^*$ .

- 5: **Compute the optimal input sequence:**

$$u^* = \tilde{U}_f g^*$$

- 6: **Apply inputs:**  $u(t), \dots, u(t+s)$  from  $u^*$  for some  $s \leq N-1$ .

- 7: **Update time step:**  $t \leftarrow t+s$ , and update  $u_{\text{ini}}$  and  $y_{\text{ini}}$  with the most recent  $T_{\text{ini}}$  measurements.

- 8: **Repeat from line 1.**
- 

Our proposed method builds on DeePC to apply data-driven control to nonlinear systems. By selecting past trajectories closest to the current operating point we implicitly leverage the idea that, locally, the nonlinear system behaves approximately linearly. This aligns with the theoretical framework of [14], which extends the *Fundamental Lemma* to affine systems and demonstrates that, under suitable assumptions, the input-output behavior of a nonlinear system can be well-approximated by its local linearization. Moreover, their results establish *practical stability guarantees* for data-driven MPC applied to nonlinear systems, ensuring that the closed-loop system remains near the optimal reachable equilibrium.

While our approach shares this fundamental insight, Contextual sampling dynamically selects relevant data rather than modifying the underlying data-driven model formulation. This raises theoretical questions about the impact of data selection on stability and robustness, particularly how the selected subset influences prediction error and long-term closed-loop performance. Future work will build on the results of [14] to investigate theoretical guarantees for Contextual sampling.

### III. CASE STUDY: MOTION PLANNING FOR AUTOMATED VEHICLES

#### A. Experiment Setup

We apply DeePC with Contextual sampling to motion planning for automated vehicles in simulation, using the F1TENTH open-source environment [20]. The vehicle dynamics follow the single-track model [21], which represents the car as a rigid body with two virtual wheels (front and rear), accounting for tire slip via the slip angle  $\beta$ . The system state consists of position, velocity, and orientation  $(x, y, v, \psi)$ , while control inputs are acceleration and steering angle  $(a, \delta)$ .

The objective is to track a reference trajectory, composed of target positions, velocity, and heading. We use the São Paulo race line from [22], a challenging track with tight turns and straight sections. The vehicle follows the path for two laps, generating local reference trajectories at each step. Optimization is solved using OSQP [23].

Table I summarizes the optimization weights and constraints, which are based on the physical limits of the F1TENTH vehicle [20]. The regularization term  $\lambda_g$  is scaled by the dimension of  $g$  for consistency.

TABLE I: Weights and constraints used in DeePC.

Parameter	Value
$R$	$\text{diag}([0.1, 1])$
$Q$	$\text{diag}([10, 10, 1, 1])$
$\lambda_g$	$\text{dim}(g) \cdot 0.1$
$\lambda_\sigma$	100
$\delta_{\min}, \delta_{\max}$	$-24, 24^\circ$
$\dot{\delta}_{\max}$	$180^\circ/\text{s}$
$v_{\min}, v_{\max}$	0, 9 m/s
$a_{\max}$	3 m/s <sup>2</sup>

To generate datasets, we run simulations with randomized inputs to ensure persistency of excitation. The steering angle is sampled uniformly from  $[-24^\circ, 24^\circ]$ , and acceleration from  $[0.0 \text{ m/s}^2, 3.0 \text{ m/s}^2]$ , updated every 0.1 s. We collect 50 s of data, yielding 500 samples. For the Hankel matrix, we set  $T_{\text{ini}} = N = 5$ , resulting in 491 sub-trajectories. To promote generalization between similar sub-trajectories, they are transformed from global to local coordinates, aligning the initial pose at  $(0, 0)$  m with a heading of  $0^\circ$ . Figure 1 illustrates the generalized data.

#### B. Results

We evaluate the open-loop prediction accuracy and the closed-loop tracking accuracy. As a baseline, we use Leverage Score sampling, which produced meaningful results in [15]. Leverage score sampling selects sub-trajectories based on their contribution to the matrix's column space, using probabilities proportional to the diagonal entries of the projection matrix onto the top singular vectors, which correspond to the left singular vectors in the truncated singular value decomposition (SVD), ensuring that the sampled sub-trajectories approximate the spectral properties of the original matrix. In contrast to Contextual sampling, Leverage Score sampling does not

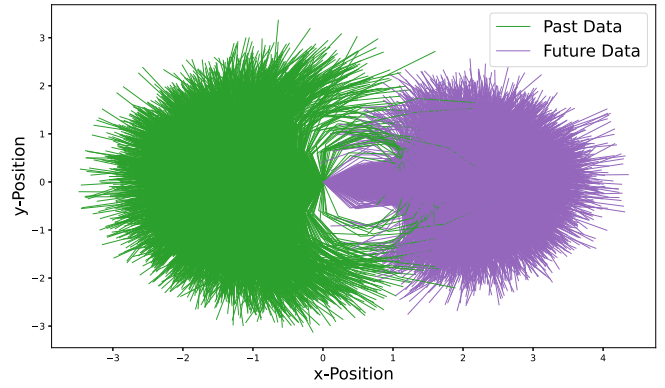


Fig. 1: Generalized trajectories.

consider the current operating point of the system. To evaluate the open-loop prediction, we collect a second trajectory for 50 s and build the corresponding test Hankel matrix containing 491 sub-trajectories. For every sub-trajectory in the test Hankel matrix, we use Contextual sampling to select the  $N_s$  closest sub-trajectories from the original Hankel matrix and build the mosaic-Hankel matrix. We solve the first three blocks of equation (3) for  $g$  and predict the future outputs  $\hat{y} = \tilde{Y}_p g$ . Last, we compute the median weighted prediction error  $\tilde{e}_{\text{pred}}$  over all  $N_{\text{exp}}$  experiments as:

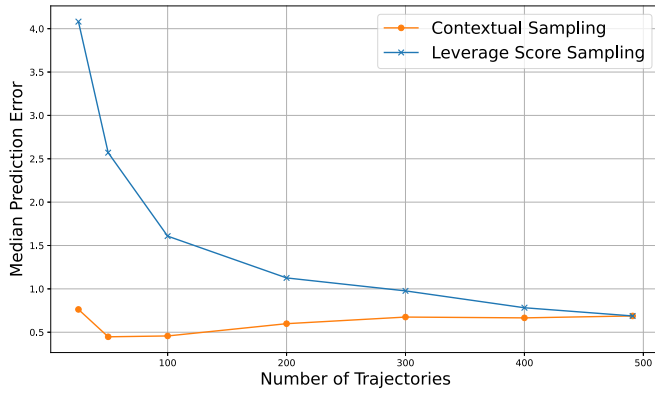
$$\tilde{e}_{\text{pred}} = \text{median} \left( \left\{ \sum_{k=1}^N \|y_{t|k} - \hat{y}_{t|k}\|_Q \mid t \in \{1, \dots, N_{\text{exp}}\} \right\} \right). \quad (9)$$

To evaluate the tracking error we simulate the vehicle for two laps and compute the median weighted tracking error over the simulation time  $T_{\text{exp}}$  as:

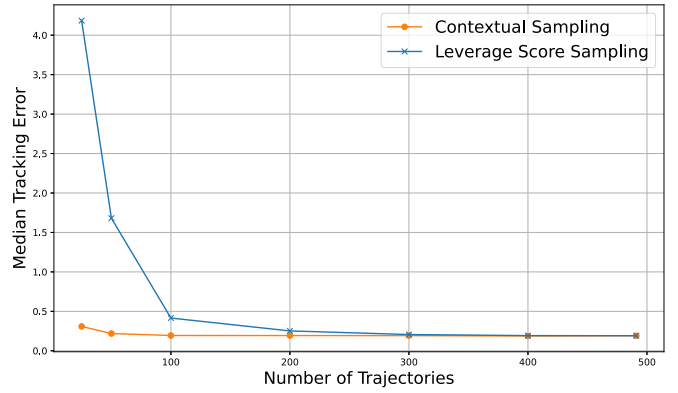
$$\tilde{e}_{\text{track}} = \text{median} \left( \left\{ \|y_t - r_t\|_Q \mid t \in \{1, \dots, T_{\text{exp}}\} \right\} \right). \quad (10)$$

We choose  $N_s \geq 25$  close to the theoretical limit of 20 for achieving persistency of excitation for  $u$ . We start with 25 sub-trajectories and increase the number to 50, to 100, and to the maximum of 491 in increments of 100. Figure 2 shows the resulting open-loop prediction and closed-loop tracking error as a function of the number of sub-trajectories for both Contextual sampling and Leverage Score sampling.

For Leverage Score sampling, the prediction error decreases as the number of samples increases, consistent with the results of [15]. This is expected since Leverage Score sampling does not consider the operating point, and increasing the number of sub-trajectories reduces overfitting to sub-trajectories far from the current operating point. For Contextual sampling, the prediction error initially decreases, reaching a minimum at  $N_s = 50$ , but then increases as more sub-trajectories are added. The initially higher prediction error can also be attributed to overfitting. However, beyond  $N_s = 50$ , adding sub-trajectories negatively impacts prediction accuracy, suggesting that only sub-trajectories close to the current operating point improve



(a) Mean prediction error as a function of the number of trajectories for Contextual sampling and Leverage Score sampling.



(b) Mean tracking error as a function of the number of trajectories for Contextual sampling and Leverage Score sampling.

Fig. 2: Comparison of mean prediction error and mean tracking error across different numbers of trajectories for Contextual sampling and Leverage Score sampling.

predictive performance. When the maximum number of sub-trajectories is used, both methods yield the same result, as they utilize the full dataset.

The tracking error follows a similar trend. For Leverage Score sampling, tracking error decreases as the number of sub-trajectories increases. In contrast, Contextual sampling achieves a 53.2% lower tracking error than Leverage Score sampling at  $N_s = 100$ , demonstrating its effectiveness in improving tracking performance with fewer sub-trajectories. Unlike prediction error, tracking error continues to improve up to  $N_s = 100$ , beyond which gains become negligible. Interestingly, despite the increase in prediction error beyond  $N_s = 50$ , tracking error remains stable and even improves. This suggests that the closed-loop control formulation compensates for prediction inaccuracies by optimizing control inputs, allowing effective tracking even with suboptimal predictions. Additionally, control regularization and feedback adaptation may smooth out errors, preventing them from significantly degrading long-term tracking performance. Thus, while adding more sub-trajectories beyond  $N_s = 100$  does not improve tracking, Contextual sampling effectively balances dataset size, prediction accuracy, and tracking robustness. Figure 3 visualizes the tracking performance of DeePC with Contextual sampling using 100 sub-trajectories.

The advantage of using fewer sub-trajectories becomes evident when evaluating computation time. Table II lists the median and maximum computation times for DeePC with Contextual sampling, measured on an Apple M3 Pro Chip with 36 GB of memory. For  $N_s \leq 100$ , the maximum computation time remains below the sampling time of 0.1 s, ensuring real-time feasibility. Notably, Contextual sampling reduces max computation time by 87.2% compared to using all 491 sub-trajectories, while maintaining comparable tracking performance. This demonstrates that fewer, well-chosen trajectories can achieve efficient and effective control. We conclude that Contextual sampling enables real-time performance with as

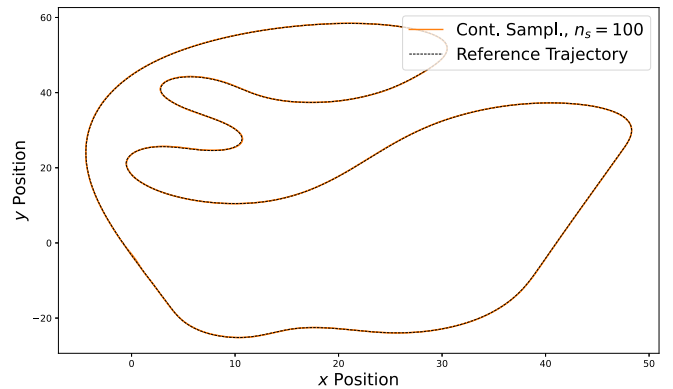


Fig. 3: Measured position vs. reference path using DeePC with Contextual sampling and 100 trajectories.

few as 100 sub-trajectories and remains viable even with just 25, albeit with a slight increase in tracking error. These findings reinforce the principle that more data is not always better—selecting the right data is key to balancing performance and efficiency in data-driven control.

TABLE II: Median and maximum computation time as a over the number of sub-trajectories for DeePC with Contextual sampling.

$N_s$	Median Comp. Time (s)	Max Comp. Time (s)
25	0.0018	0.0248
50	0.0024	0.0394
100	0.0025	0.0692
200	0.0035	0.1543
300	0.0044	0.2723
400	0.0053	0.4154
491	0.0038	0.5246

### C. Discussion

Although our results highlight the advantages of Contextual sampling in improving computational efficiency and tracking accuracy compared to leverage score sampling, our approach also has limitations, which we discuss here. The Contextual sampling method does not guarantee that the resulting mosaic-Hankel matrix is collectively persistently exciting. Furthermore, while reducing the size of the dataset used within DeePC reduces computation time and tracking error in our case study, a sufficiently large total dataset remains necessary to ensure that diverse system behaviors are available for selection. Related to this, accurately approximating the current dynamics of the system requires the current operating point to be well represented in the total dataset. This reliance on dataset quality is a notable disadvantage compared to methods that exploit global linearity in higher dimensions, where learned nonlinear mappings can generalize beyond the collected data.

### IV. CONCLUSION

This work introduced Contextual Trajectory sampling, a data-driven approach that enhances DeePC for nonlinear systems by dynamically selecting the most relevant sub-trajectories based on the current operating point. By leveraging fewer but relevant data points, our method significantly improves computational efficiency while maintaining high tracking accuracy. Our evaluation in an automated vehicle motion planning scenario demonstrated that “less is more”—Contextual sampling achieves tracking performance comparable to MPC, yet requires fewer sub-trajectories and significantly reduces computation time. Notably, we showed that reducing the dataset size not only improves real-time feasibility but can also enhance prediction accuracy, as the selected data better captures the system’s current dynamics. However, the method has limitations that warrant further investigation. Contextual sampling does not inherently guarantee collective persistency of excitation, and its effectiveness depends on the dataset’s diversity and coverage of relevant system behaviors. Future research should explore strategies to ensure persistency while maintaining computational efficiency, as well as extend the approach to more complex, high-dimensional systems. These findings highlight the potential of Contextual sampling as an efficient and scalable approach for data-driven control, reinforcing the idea that more data is not always better—selecting the right data is key.

### REFERENCES

- [1] E. F. Camacho and C. Bordons, *Model Predictive control*, ser. Advanced Textbooks in Control and Signal Processing, M. J. Grimble and M. A. Johnson, Eds. London: Springer London, 2007.
- [2] P. Scheffe, T. M. Henneken, M. Kloock, and B. Alrifaae, “Sequential Convex Programming Methods for Real-Time Optimal Trajectory Planning in Autonomous Vehicle Racing,” *IEEE Transactions on Intelligent Vehicles*, vol. 8, no. 1, pp. 661–672, Jan. 2023.
- [3] B. Alrifaae and J. Maczajewski, “Real-time Trajectory optimization for Autonomous Vehicle Racing using Sequential Linearization,” in *2018 IEEE Intelligent Vehicles Symposium (IV)*. Changshu: IEEE, Jun. 2018, pp. 476–483.
- [4] J. Coulson, J. Lygeros, and F. Dörfler, “Data-Enabled Predictive Control: In the Shallows of the DeePC,” in *2019 18th European Control Conference (ECC)*. Naples, Italy: IEEE, Jun. 2019, pp. 307–312.
- [5] J. Berberich and F. Allgöwer, “An Overview of Systems-Theoretic Guarantees in Data-Driven Model Predictive Control,” *Annual Review of Control, Robotics, and Autonomous Systems*, Oct. 2024.
- [6] J. Berberich and F. Allgöwer, “A trajectory-based framework for data-driven system analysis and control,” in *2020 European Control Conference (ECC)*. Saint Petersburg, Russia: IEEE, May 2020, pp. 1365–1370.
- [7] J. G. Rueda-Escobedo and J. Schiffer, “Data-Driven Internal Model Control of Second-Order Discrete Volterra Systems,” in *2020 59th IEEE Conference on Decision and Control (CDC)*. Jeju, Korea (South): IEEE, Dec. 2020, pp. 4572–4579.
- [8] V. K. Mishra, I. Markovsky, A. Fazzi, and P. Dreesen, “Data-Driven Simulation for NARX Systems,” in *2021 29th European Signal Processing Conference (EUSIPCO)*. Dublin, Ireland: IEEE, Aug. 2021, pp. 1055–1059.
- [9] Y. Lian, Y. Lian, and E. Ch, “Nonlinear Data-Enabled Prediction and Control,” *Proceedings of Machine Learning Research*, 2021.
- [10] Y. Lian, R. Wang, and C. N. Jones, “Koopman based data-driven predictive control,” 2021, version Number: 2.
- [11] L. Huang, J. Lygeros, and F. Dörfler, “Robust and Kernelized Data-Enabled Predictive Control for Nonlinear Systems,” *IEEE Transactions on Control Systems Technology*, vol. 32, no. 2, pp. 611–624, Mar. 2024.
- [12] M. Lazar, “Basis-Functions Nonlinear Data-Enabled Predictive Control: Consistent and Computationally Efficient Formulations,” in *2024 European Control Conference (ECC)*. Stockholm, Sweden: IEEE, Jun. 2024, pp. 888–893.
- [13] —, “Neural data-enabled predictive control,” *IFAC-PapersOnLine*, vol. 58, no. 15, pp. 91–96, 2024, 20th IFAC Symposium on System Identification SYSID 2024.
- [14] J. Berberich, J. Kohler, M. A. Muller, and F. Allgöwer, “Linear Tracking MPC for Nonlinear Systems—Part II: The Data-Driven Case,” *IEEE Transactions on Automatic Control*, vol. 67, no. 9, pp. 4406–4421, Sep. 2022.
- [15] L. Schmitt, J. Beerwerth, and D. Abel, “Data selection and data-enabled predictive control for a fuel cell system,” *IFAC-PapersOnLine*, vol. 56, no. 2, pp. 4436–4441, 2023.
- [16] I. Markovsky and Society for Industrial and Applied Mathematics, Eds., *Exact and approximate modeling of linear systems: a behavioral approach*, ser. Mathematical modeling and computation. Philadelphia, Pa: Society for Industrial and Applied Mathematics (SIAM, 3600 Market Street, Floor 6, Philadelphia, PA 19104), 2006, no. 11.
- [17] J. C. Willems, P. Rapisarda, I. Markovsky, and B. L. De Moor, “A note on persistency of excitation,” *Systems & Control Letters*, vol. 54, no. 4, pp. 325–329, Apr. 2005.
- [18] J. Coulson, J. Lygeros, and F. Dörfler, “Distributionally Robust Chance Constrained Data-Enabled Predictive Control,” *IEEE Transactions on Automatic Control*, vol. 67, no. 7, pp. 3289–3304, Jul. 2022.
- [19] H. J. Van Waarde, C. De Persis, M. K. Camlibel, and P. Tesi, “Willems’ Fundamental Lemma for State-Space Systems and Its Extension to Multiple Datasets,” *IEEE Control Systems Letters*, vol. 4, no. 3, pp. 602–607, Jul. 2020.
- [20] M. O’Kelly, H. Zheng, D. Karthik, and R. Mangharam, “F1tenth: An open-source evaluation environment for continuous control and reinforcement learning,” *Proceedings of Machine Learning Research*, vol. 123, 2019.
- [21] M. Althoff, M. Koschi, and S. Manzingler, “CommonRoad: Composable benchmarks for motion planning on roads,” in *2017 IEEE Intelligent Vehicles Symposium (IV)*. Los Angeles, CA, USA: IEEE, Jun. 2017, pp. 719–726.
- [22] J. Betz, H. Zheng, A. Liniger, U. Rosolia, P. Karle, M. Behl, V. Kroví, and R. Mangharam, “Autonomous Vehicles on the Edge: A Survey on Autonomous Vehicle Racing,” *IEEE Open Journal of Intelligent Transportation Systems*, vol. 3, pp. 458–488, 2022.
- [23] B. Stellato, G. Banjac, P. Goulart, A. Bemporad, and S. Boyd, “OSQP: an operator splitting solver for quadratic programs,” *Mathematical Programming Computation*, vol. 12, no. 4, pp. 637–672, Dec. 2020.